A&A 518, L35 (2010)
DOI: 10.1051/0004-6361/201014548

Herschel: the first science highlights

Astronomy & Astrophysics
Special feature

LETTER TO THE EDITOR

Herschel and SCUBA-2 imaging and spectroscopy of a bright, lensed submillimetre galaxy at $z = 2.3^{\star}$

R. J. Ivison[1,2], A. M. Swinbank[3], B. Swinyard[4], I. Smail[3], C. P. Pearson[4,5], D. Rigopoulou[4,6], E. Polehampton[4,5], J.-P. Baluteau[7], M. J. Barlow[8], A. W. Blain[9], J. Bock[9,10], D. L. Clements[11], K. Coppin[3], A. Cooray[12], A. Danielson[3], E. Dwek[13], A. C. Edge[3], A. Franceschini[14], T. Fulton[15], J. Glenn[16], M. Griffin[17], K. Isaak[17], S. Leeks[4], T. Lim[4], D. Naylor[5], S. J. Oliver[18], M. J. Page[19], I. Pérez Fournon[20,21], M. Rowan-Robinson[10], G. Savini[22], D. Scott[23], L. Spencer[17], I. Valtchanov[24], L. Vigroux[25], and G. S. Wright[1]

(Affiliations are available in the online edition)

Received 30 March 2010 / Accepted 20 April 2010

ABSTRACT

We present a detailed analysis of the far-infrared (-IR) properties of the bright, lensed, $z = 2.3$, submillimetre-selected galaxy (SMG), SMM J2135−0102 (hereafter SMM J2135), using new observations with *Herschel*, SCUBA-2 and the Very Large Array (VLA). These data allow us to constrain the galaxy's spectral energy distribution (SED) and show that it has an intrinsic rest-frame 8−1000-μm luminosity, $L_{\rm bol}$, of $(2.3 \pm 0.2) \times 10^{12}\ L_{\odot}$ and a likely star-formation rate (SFR) of $\sim$400 $M_{\odot}$ yr^{-1}. The galaxy sits on the far-IR/radio correlation for far-IR-selected galaxies. At $\gtrsim$70 μm, the SED can be described adequately by dust components with dust temperatures, $T_{\rm d} \sim 30$ and 60 K. Using SPIRE's Fourier-transform spectrometer (FTS) we report a detection of the [C II] 158 μm cooling line. If the [C II], CO and far-IR continuum arise in photodissociation regions (PDRs), we derive a characteristic gas density, $n \sim 10^3$ cm^{-3}, and a far-ultraviolet (-UV) radiation field, G_0, $10^3\times$ stronger than the Milky Way. $L_{\rm [CII]}/L_{\rm bol}$ is significantly higher than in local ultra-luminous IR galaxies (ULIRGs) but similar to the values found in local star-forming galaxies and starburst nuclei. This is consistent with SMM J2135 being powered by starburst clumps distributed across $\sim$2 kpc, evidence that SMGs are not simply scaled-up ULIRGs. Our results show that SPIRE's FTS has the ability to measure the redshifts of distant, obscured galaxies via the blind detection of atomic cooling lines, but it will not be competitive with ground-based CO-line searches. It will, however, allow detailed study of the integrated properties of high-redshift galaxies, as well as the chemistry of their interstellar medium (ISM), once more suitably bright candidates have been found.

Key words. galaxies: evolution – infrared: galaxies – infrared: ISM – radio continuum: galaxies – submillimeter: galaxies

1. Introduction

Submillimetre (submm) surveys have uncovered a population of intrinsically luminous, but highly obscured, galaxies at high redshift. However, even with instrinsic luminosities of $\sim 10^{13}\ L_{\odot}$ (e.g. Ivison et al. 1998), the brightest SMGs are still challenging targets for observational studies. In the submm and far-IR, where the bulk of their luminosity escapes, the brightest SMGs have observed flux densities of only $\sim$10 mJy at 850 μm, peaking at $\sim$50 mJy at the wavelengths probed by *Herschel*. To alleviate this photon starvation, submm surveys often exploit gravitational lensing via massive, foreground galaxy clusters, thereby enhancing the apparent brightness of SMGs at all wavelengths (e.g. Smail et al. 1997; Chapman et al. 2002; Cowie et al. 2002).

Recently, Swinbank et al. (2010) exploited the cluster lensing technique using the Large Apex BOlometer CAmera (LABOCA – Siringo et al. 2009) on the 12-m Atacama Pathfinder Experiment (APEX) telescope to map the cluster, MACS J2135−01 ($z = 0.325$), and thereby discovered SMM J2135, an SMG with $S_{870\,\mu{\rm m}} = 106$ mJy. Its brightness is due to very high amplification (by 32.5 ± 4.5) by the foreground cluster (similarly bright sources may have recently been unearthed by the South Pole Telescope – Vieira et al. 2010). The lens model for SMM J2135 is well constrained and its redshift ($z = 2.3259 \pm 0.0001$, derived from the detection of CO $J = 1$–0 in a blind search) and intrinsic flux (3.3 ± 0.5 mJy) are typical of SMGs found close to the confusion limit in submm surveys. SMM J2135 thus presents an opportunity to study a member of this important population at high signal-to-noise and with the spatial and spectral resolution necessary to determine the detailed far-IR spectral properties of SMGs. Due to the high magnification, it is feasible to apply some of the observational tools used on local star-forming galaxies to understand the processes of star formation at high redshift. Indeed, we can employ diagnostics capable of determining the flux of ionising radiation and the SFR, thus determining the state of the overwhelming majority of the atomic and molecular gas in this galaxy (Wolfire et al. 1990; Hollenbach & Tielens 1999; Kaufman et al. 1999).

In this paper we present spectroscopic and photometric far-IR/submm measurements of SMM J2135 made using *Herschel* (Pilbratt et al. 2010). We also include new observations with

* *Herschel* is an ESA space observatory with science instruments provided by European-led Principal Investigator consortia and with important participation from NASA.

the James Clerk Maxwell Telescope (JCMT) and VLA. We use these observations to constrain the SED of SMM J2135 and measure or set firm limits for the line fluxes from the main atomic cooling lines.

2. Observations

To complement the existing submm photometry of SMM J2135, observations at 250, 350 and 500 μm were obtained with SPIRE (Griffin et al. 2010). The field was observed first using the "small-map mode", where orthogonal scans produce a useful cross-linked area of ∼16 arcmin^2. We used four repetitions, giving an on-source integration time of ∼200 s. Processing relied on the SPIRE scan map pipeline (Griffin et al. 2008), which deglitches, flux calibrates and performs various corrections. After removal of a linear baseline, images were made using the standard naive mapper within the *Herschel* interactive pipeline environment (HIPE v2.0). From the final maps, we identify a ∼100-σ source at the position of SMM J2135 in all bands; its flux densities are listed in Table 1.

SMM J2135 was also observed for 7 ks using the central pixels of SPIRE's FTS (covering $\lambda_{\rm obs}$ = 197–670 μm) on 2009 December 9, to search for [C II] 158 μm, redshifted to 524 μm. Even with the benefit of extreme amplification, SMM J2135 represents an extremely faint target in the context of the SPIRE spectrometer: the standard pipeline reduction shows significant problems with the overall flux level in both the high- and low-frequency channels (SSW, SLW). Rather than rely on the pipeline, we used the variation in bolometer temperature to transform the source and dark interferograms into spectra which were then subtracted and divided by a calibration spectrum of Uranus (rather than the much fainter asteroid, Vesta – see Swinyard et al. 2010). Variations in instrument temperature between the observations of the dark sky and the source can cause large relative variations in the SLW spectrum. Here, we determined the overall net flux of the source, with no subtraction or addition of flux from the variation in instrument temperature. We then inspected the SLW data and compared to the spectrum expected from the subtraction of two blackbodies at the temperatures recorded in the housekeeping data. The difference in model instrument temperatures in the dark sky and the source observation are therefore varied (by less than 1%) until a match between the overall flux level from the photometer and SSW is achieved.

New observations were also carried out with the Submillimetre Common-User Bolometer Array-2 (SCUBA-2 – Holland et al. 2006), a large-format bolometer camera for the JCMT, designed to produce simultaneous continuum images at 450 and 850 μm. These data were obtained during 2009 November 29, during early commissioning, with one 32 × 40 transition-edge sensor (TES) array at each of 450 and 850 μm, giving a field of view of ∼3′ × 3.5′ (the final commissioned instrument will have four such arrays at each wavelength). The total integration time was 3.6 ks. Pointing checks and flux calibration was achieved via observations of Neptune and Uranus, immediately before and after the science exposures. Data reduction was carried out using the SubMillimeter User Reduction Facility (SMURF), which flat-fields and stacks the images, and removes atmospheric emission. Measured flux densities are listed in Table 1.

To determine the radio properties of the galaxy, observations with the VLA were obtained during late 2009. SMM J2135 was observed in the *C* and *X* bands for 10 and 5 ks, respectively. The *C*-band observations were taken in spectral-line mode, to search for redshifted 22-GHz water maser emission, though only continuum was detected; continuum emission was also detected convincingly in the *X* band (Table 1).

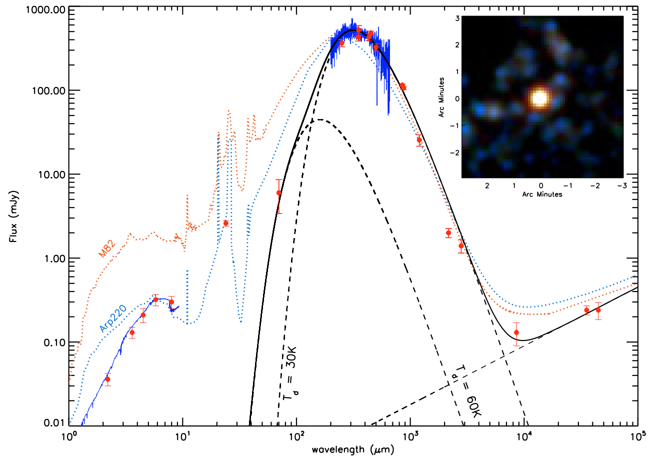

Fig. 1. The rest-frame near-IR-radio SED of SMM J2135, with new *Herschel*, SCUBA-2 and VLA observations complementing existing photometry (Swinbank et al. 2010). The FTS spectrum is shown in blue. In the rest-frame optical to mid-IR regime, SMM J2135 is less luminous than Arp 220 and considerably fainter than M 82, possibly reflecting strong dust obscuration. We model the SED using a two-component dust model (solid, black line) comprising two modified blackbodies (β = +2.0) with $T_{\rm d}$ = 30 and 60 K. The solid blue line denotes a stellar fit to the rest-frame UV-near-IR photometry. Inset is a colour image, centred on SMM J2135, generated from the SPIRE 250-, 350- and 500-μm observations (N, up; E, *left*).

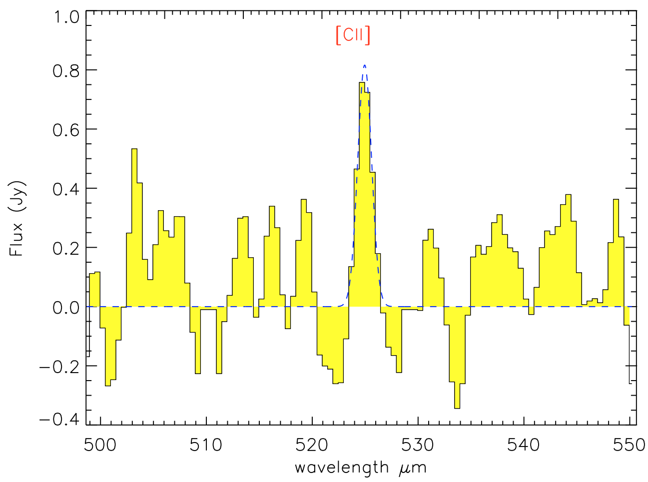

Fig. 2. Region around the redshifted [C II] 158 μm, the strongest atomic fine-structure line detected by our FTS spectrum of SMM J2135. Dashed line: best Gaussian fit, with $v_{\rm lsr}$ = −180 ± 150 km s^{-1}, which corresponds to strong components in the HCN, C I and CO lines (Danielson et al., in preparation). Using the line flux and following Eq. (1) of Hailey-Dunsheath et al. (2010), we estimate a gas mass, $M_{\rm [CII]}$ ∼ 4 × 10^9 $M_\odot$, which is ∼25% of the total molecular gas mass, similar to the ratio found in local starburst galaxies (Stacey et al. 1991).

3. Analysis and discussion

3.1. Far-infrared SED

The new observations clearly identify a turnover in the SED of SMM J2135 at ∼350 μm (Fig. 1). We use the far-IR photometry (Table 1 and Swinbank et al. 2010) to calculate its rest-frame 8−1000-μm luminosity directly, which is due largely to

Table 1. Photometry.

Wavelength	Flux[a] (mJy)	Observatory/Instrument
250 μm	366 ± 55	*Herschel*/SPIRE
350 μm	429 ± 64	*Herschel*/SPIRE
352 μm	520 ± 70	APEX/SABOCA[b]
434 μm	430 ± 40	SMA[b]
450 μm	480 ± 54	SCUBA-2
500 μm	325 ± 49	*Herschel*/SPIRE
850 μm	115 ± 13	SCUBA-2
870 μm	106 ± 12	APEX/LABOCA[b]
1.2 mm	26 ± 4	SMA[b]
2.17 mm	2.0 ± 0.25	PdBI[b]
2.80 mm	1.4 ± 0.25	PdBI[b]
8.57 mm	0.13 ± 0.05	GBT/Zpectrometer[b]
3.55 cm	0.240 ± 0.030	VLA/X
4.49 cm	0.240 ± 0.055	VLA/C

Notes. [(a)] Errors include uncertainty in absolute flux calibration; [(b)] see Swinbank et al. (2010), also for $\lambda_{\rm obs} < 250\,\mu$m.

dust-reprocessed UV light and provides a measure of its instantaneous SFR. Correcting for lensing amplification, we find $L_{\rm bol} = (2.3 \pm 0.2) \times 10^{12}\ L_\odot$, indicating a SFR of $\sim$400 $M_\odot$ yr^{-1} (Kennicutt 1998). $L_{\rm bol}$ is thus comparable to that of Arp 220 and rather higher than that quoted by Swinbank et al. (2010) who integrated the best modified blackbody fit to the 350-, 434- and 870-μm emission, missing much of the energy at rest-frame $\sim$8−100 μm.

If we parameterise the far-IR SED of SMM J2135 using a modified blackbody spectrum, a single component model with $T_{\rm d}$ = 34 K underestimates $S_{70\mu{\rm m}}$ by $\sim$100×. A two-component model with $T_{\rm d}$ = 30 and 60 K provides a significantly improved fit (Fig. 1). The mass of dust associated with the warm and cool components are $M_{\rm d}^{\rm warm} = 10^6$ and $M_{\rm d}^{\rm cool} = 4 \times 10^8\ M_\odot$ (adopting the parameters used by Dunne et al. 2000). Given the cold molecular gas mass derived from the CO(1−0) emission ($M_{\rm gas} = (16 \pm 1) \times 10^9\ M_\odot$ – Swinbank et al. 2010), this suggests a gas-to-dust ratio of $M_{\rm gas}/M_{\rm d} \sim 40$, rather lower than that of the Milky Way, 120, and Lyman-break galaxies ($\sim$100; e.g. Coppin et al. 2007) but consistent with typical SMGs ($\sim$60; e.g. Coppin et al. 2008) given that the uncertainties are considerable.

3.2. Radio properties

If the radio spectrum of SMM J2135 follows a $S_\nu \propto \nu^{-0.7}$ power law, which is consistent with the data but by no means certain (Fig. 1; Table 1), then its radio luminosity is $L_{1.4\ \rm GHz} = 9 \times 10^{23}$ W Hz^{-1} so that $q_{\rm IR}$ = 2.42 ± 0.06, entirely consistent with the far-IR/radio correlation for 250-μm-selected galaxies ($\langle q_{\rm IR}\rangle$ = 2.40 – Ivison et al. 2010a).

3.3. Spectral properties

The full FTS spectrum (Fig. 1) covers the major fine-structure cooling lines and we detect one strong emission line, [C II]λ158 μm, at the 4.3-σ level (Fig. 2). Table 2 presents the best-fit flux with the width constrained to the instrumental resolution. The flux is not sensitive to the fit parameters, for example returning values well within 1σ for a line fixed at $v_{\rm lsr}$ = 0 km s^{-1}. The FTS spectrum covers several other lines and although we see hints of emission associated with [O I]λ145 μm and [N II]λ122 μm, we have chosen to report conservative upper limits (best-bet flux plus 3σ) on these and other lines in Table 2.

Table 2. Spectral-line and bolometric luminosities.

Line	$\lambda_{\rm rest}$ (μm)	Flux[a] ($\times 10^{-17}$ W m^{-2})	Luminosity ($L_\odot$)
[O I]	63.18	$3\sigma < 4.5$	$3\sigma < 14.9 \times 10^9$
[O III]	88.36	$3\sigma < 2.4$	$3\sigma < 8.0 \times 10^9$
[N II]	122.10	$3\sigma < 1.4$	$3\sigma < 4.7 \times 10^9$
[O I]	145.53	$3\sigma < 2.5$	$3\sigma < 8.5 \times 10^9$
[C II]	157.74	1.7 ± 0.4	$(5.5 \pm 1.3) \times 10^9$
CO(1−0)	2602.6	2.14 ± 0.12[b]	$(8.0 \pm 0.4) \times 10^5$
$L_{\rm bol}$	...	...	$(2.3 \pm 0.2) \times 10^{12}$

Notes. [(a)] Line width constrained to instrumental resolution; [(b)] Jy km s^{-1}.

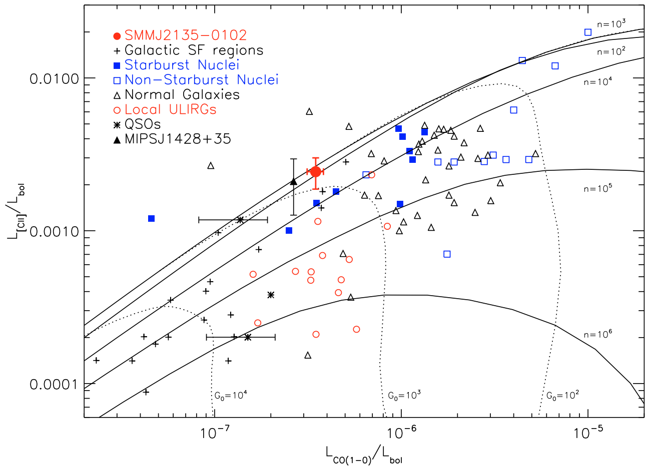

Fig. 3. $L_{\rm [CII]}/L_{\rm bol}$ versus $L_{\rm CO(1-0)}/L_{\rm bol}$ for SMM J2135 compared to star-forming regions, star-forming galaxies and ULIRGs in the local Universe. This figure is adapted from Hailey-Dunsheath et al. (2010) and shows the ratios for powerful, high-redshift QSOs as well as the SMG, MIPS J1428+35. Tracks for PDR models of gas density, n, and far-UV field strength, G_0, are taken from Kaufman et al. (1999). We see that the gas in SMM J2135 experiences a far-UV field similar to that seen in local ULIRGs, but is at much lower densities than the typical material in such systems.

[C II] is one of the brightest emission lines in star-forming galaxies, typically accounting for 0.1−1% of $L_{\rm bol}$. It arises from the warm and dense PDRs that form on the UV-illuminated surfaces of molecular clouds, though the [C II] flux from diffuse H II regions or from diffuse PDRs can be considerable (e.g. Madden et al. 1993; Lord et al. 1996). In local star-forming galaxies, $L_{\rm [C\,II]}/L_{\rm bol}$ and $L_{\rm [CII]}/L_{\rm CO(1-0)}$ provide a sensitive test of the physical conditions within the ISM. For SMM J2135 we find $L_{\rm [CII]}/L_{\rm bol} = (2.4 \pm 0.6) \times 10^{-3}$ and $L_{\rm CO(1-0)}/L_{\rm bol} = (3.5 \pm 0.5) \pm \times 10^{-7}$ and compare these to measurements of local galaxy populations in Fig. 3. We see that $L_{\rm [CII]}/L_{\rm CO(1-0)}$ in SMM J2135 is similar to local ULIRGs, but that $L_{\rm CO(1-0)}/L_{\rm bol}$ is consistent with the ratios found in more typical star-forming galaxies and nuclei.

The [C II] transition is a primary PDR coolant and is a sensitive probe of both the physical conditions of the photo-dissociated gas and the intensity of the ambient stellar radiation field (Hollenbach & Tielens 1999). Hence using the PDR models of Kaufman et al. (1999) we can determine an acceptable range of temperature, T, and gas density, n, in SMM J2135, from our measurements of [C II], CO(1−0) and $L_{\rm bol}$. In these models, $L_{\rm [CII]}/L_{\rm CO(1-0)}$ is most sensitive to n whilst $L_{\rm [CII]}/L_{\rm bol}$ is sensitive to the incident far-UV field strength, G_0, and hence T. Figure 3 shows $L_{[CII]}/L_{bol}$ versus L_{CO1-0}/L_{bol} and suggests a best-fit density, $n \sim 10^3$ cm^{-3}, with $T \sim 400$ K and $G_0 \sim 10^3$ (Kaufman et al. 1999). G_0 is measured in multiples of the local interstellar value, so the far-UV radiation field illuminating the PDRs is $\sim 10^3\times$ more intense than that in the Milky Way, but comparable to that found in local ULIRGs and the $z = 1.3$ SMG, MIPS J1428 (Hailey-Dunsheath et al. 2010), while the densities in SMM J2135 ($n \sim 10^3$) are most similar to those found in normal star-forming galaxies, 10−100× lower than those seen in local ULIRGs.

Taken together, this suggests that the molecular emission does not reside in a single, compact region, illuminated by an intense UV radiation field, but that the material is more extended, with the high $L_{[CII]}/L_{bol}$ ratio then reflecting the lower density of this extended medium. Indeed, Swinbank et al. (2010) show that although the rest-frame 260-μm emission is dominated by four star-forming regions, each ~100 pc across, the emission extends over ~2 kpc. The size of the star-forming region in SMM J2135 is also comparable to the sizes of the dense gas reservoirs inferred from high-J CO mapping, ~3 kpc (Tacconi et al. 2008). Thus SMM J2135 appears to be powered by an intense starburst whose influence is felt over a larger region than those seen in local ULIRGs, as has been suggested for SMGs using radio, submm and CO sizes (Biggs & Ivison 2008; Younger et al. 2008; Biggs et al. 2010; Ivison et al. 2010b), near- and mid-IR colours and spectra (Hainline et al. 2009; Menéndez-Delmestre et al. 2009) and other far-IR spectroscopy (Hailey-Dunsheath et al. 2010).

4. Discussion and conclusions

We have delineated the far-IR SED of a highly magnified (but intrinsically typical) SMG, SMM J2135, at $z = 2.3$. Its rest-frame 8−1000-μm and 1.4-GHz luminosities are 2.3×10^{12} $L_\odot$ and 9×10^{23} W Hz^{-1}, with $SFR \sim 400$ $M_\odot$ yr^{-1}, and it sits on the far-IR/radio correlation for starburst galaxies.

Herschel FTS spectroscopy detects the redshifted [C II] 158 μm emission line, allowing us to investigate the properties of its ISM. The line luminosity suggests that the mass of [C II] is ~25% of the molecular gas, similar to the ratio found in local starbursts.

We use CO(1–0), [C II] and L_{bol} to investigate the ISM's physical conditions. From a comparison with PDR models, we derive a far-UV radiation field, G_0, which is $\sim 10^3\times$ higher than that in the Milky Way, but comparable to those found in ULIRGs. In contrast, we find a characteristic density, $n \sim 10^3$ cm^{-3}, which is lower than seen in ULIRGs, but comparable to values seen in local star-forming galaxies and nuclei, as well as a small number of high-redshift systems where similar measurements have been made. Together these results suggest that SMM J2135 has a SFR intensity similar to that seen in local ULIRGs, but distributed over a larger volume. This is consistent with the ~2-kpc distribution of star formation across this galaxy (Swinbank et al. 2010) and previous suggestions of extended star formation in SMGs (e.g. Biggs & Ivison 2008).

Our results show that SPIRE's FTS has the ability to measure the redshifts of suitably bright and distant, obscured galaxies via detection of atomic cooling lines such as [C II]. However, we estimate that ≳10-h integrations will be required and this is not competitive with blind, ground-based CO-line searches (e.g. Weiß et al. 2009), as evidenced by the ease with which the redshift of SMM J2135 was determined using Zpectrometer on the Green Bank Telescope (Swinbank et al. 2010). Nevertheless, our results show that facilities such as *Herschel* and SCUBA-2 will allow detailed study of the integrated properties of high-redshift galaxies (through SED modelling), as well as the chemistry of their ISM.

Acknowledgements. We thank Steve Hailey-Dunsheath for useful discussion. We thank Fred Lo for granting DDT observations, and Wayne Holland for observing SMM J2135 during SCUBA-2 commissioning. SPIRE has been developed by a consortium of institutes led by Cardiff Univ. (UK) and including Univ. Lethbridge (Canada); NAOC (China); CEA, LAM (France); IFSI, Univ. Padua (Italy); IAC (Spain); Stockholm Observatory (Sweden); Imperial College London, RAL, UCL-MSSL, UKATC, Univ. Sussex (UK); Caltech, JPL, NHSC, Univ. Colorado (USA). This development has been supported by national funding agencies: CSA (Canada); NAOC (China); CEA, CNES, CNRS (France); ASI (Italy); MCINN (Spain); SNSB (Sweden); STFC (UK); and NASA (USA). SCUBA-2 is funded by STFC, the JCMT Development Fund and the Canadian Foundation for Innovation.

References

Biggs, A. D., & Ivison, R. J. 2008, MNRAS, 385, 893
Biggs, A. D., Younger, J. D., & Ivison, R. J. 2010, MNRAS, in press [arXiv:1004.0009]
Chapman, S. C., Scott, D., Borys, C., & Fahlman, G. G. 2002, MNRAS, 330, 92
Coppin, K., Swinbank, A. M., Neri, R., et al. 2008, MNRAS, 389, 45
Coppin, K., Swinbank, A. M., Neri, R., et al. 2007, ApJ, 665, 936
Cowie, L. L., Barger, A. J., & Kneib, J. 2002, AJ, 123, 2197
Dunne, L., Eales, S., Edmunds, M., et al. 2000, MNRAS, 315, 115
Griffin, M., Dowell, C. D., Lim, T., et al. 2008, in SPIE Conf. Ser., 7010
Griffin, M. J., Abergel, A., Abreu, A., et al. 2010, A&A, 518, L3
Hailey-Dunsheath, S., Nikola, T., Stacey, G. J., et al. 2010, ApJ, 714, L162
Hainline, L. J., Blain, A. W., Smail, I., et al. 2009, ApJ, 699, 1610
Holland, W., MacIntosh, M., Fairley, A., et al. 2006, in SPIE Conf. Ser., 6275
Hollenbach, D. J., & Tielens, A. G. G. M. 1999, Rev. Mod. Phys., 71, 173
Ivison, R. J., Smail, I., Le Borgne, J., et al. 1998, MNRAS, 298, 583
Ivison, R. J., Magnelli, B., Ibar, E., et al. 2010a, A&A, 518, L31
Ivison, R. J., Smail, I., Papadopoulos, P. P., et al. 2010b, MNRAS, 404, 198
Kaufman, M. J., Wolfire, M. G., Hollenbach, D. J., & Luhman, M. L. 1999, ApJ, 527, 795
Kennicutt, Jr., R. C. 1998, ARA&A, 36, 189
Lord, S. D., Malhotra, S., Lim, T., et al. 1996, A&A, 315, L117
Madden, S. C., Geis, N., Genzel, R., et al. 1993, ApJ, 407, 579
Menéndez-Delmestre, K., Blain, A. W., Smail, I., et al. 2009, ApJ, 699, 667
Pilbratt, G. L., Riedinger, J. R., Passvogel, T., et al. 2010, A&A, 518, L1
Siringo, G., Kreysa, E., Kovács, A., et al. 2009, A&A, 497, 945
Smail, I., Ivison, R. J., & Blain, A. W. 1997, ApJ, 490, L5
Stacey, G. J., Geis, N., Genzel, R., et al. 1991, ApJ, 373, 423
Swinbank, A. M., Smail, I., Longmore, S., et al. 2010, Nature, 464, 733
Swinyard, B., Ade, P., Baluteau J. P. et al. 2010, A&A, 518, L4
Tacconi, L. J., Genzel, R., Smail, I., et al. 2008, ApJ, 680, 246
Vieira, J. D., Crawford, T., Switzer, E., et al. 2010, ApJ, submitted [arXiv:0912.2338]
Weiß, A., Ivison, R. J., Downes, D., et al. 2009, ApJ, 705, L45
Wolfire, M. G., Tielens, A., & Hollenbach, D. 1990, ApJ, 358, 116
Younger, J. D., Fazio, G. G., Wilner, D. J., et al. 2008, ApJ, 688, 59

Page 5 is available in the electronic edition of the journal at http://www.aanda.org

[1] UK Astronomy Technology Centre, Royal Observatory, Blackford Hill, Edinburgh EH9 3HJ, UK
e-mail: rji@roe.ac.uk
[2] Institute for Astronomy, University of Edinburgh, Royal Observatory, Blackford Hill, Edinburgh EH9 3HJ, UK
[3] Institute for Computational Cosmology, Durham University, South Road, Durham DH1 3LE, UK
[4] Space Science & Technology Department, Rutherford Appleton Laboratory, Chilton, Didcot OX11 0QX, UK
[5] Institute for Space Imaging Science, University of Lethbridge, Lethbridge, Alberta T1K 3M4, Canada
[6] Astrophysics, Oxford University, Keble Road, Oxford, OX1 3RH, UK
[7] Observatoire Astronomique de Marseille-Provence, 2 Pl Le Verrier, 13248, Marseille, Cedex 04, France
[8] Department of Physics and Astronomy, University College London, Gower Street, London WC1E 6BT, UK
[9] California Institute of Technology, 1200 E. California Blvd, Pasadena, CA 91125, USA
[10] Jet Propulsion Laboratory, Pasadena, California 91109-8099, USA
[11] Astrophysics Group, Imperial College, Blackett Laboratory, Prince Consort Road, London SW7 2AZ, UK
[12] Center for Cosmology, Department of Physics and Astronomy, University of California, Irvine, CA 92697, USA
[13] Observational Cosmology Laboratory, Code 665, NASA Goddard Space Flight Center, Greenbelt, MD 20771, USA
[14] Dipartimento di Astronomia, Universita' di Padova, vic. Osservatorio, 3, 35122 Padova, Italy
[15] Blue Sky Spectroscopy, Lethbridge, Alberta, Canada
[16] Department of Astrophysical and Planetary Sciences, CASA 389-UCB, University of Colorado, Boulder, CO 80309, USA
[17] Cardiff School of Physics and Astronomy, Cardiff University, Queens Buildings, The Parade, Cardiff CF24 3AA, UK
[18] Astronomy Centre, Department of Physics & Astronomy, University of Sussex, Falmer, East Sussex BN1 9QH, UK
[19] Mullard Space Science Laboratory, University College London, Holmbury St Mary, Dorking, Surrey RH5 6NT, UK
[20] Instituto de Astrofísica de Canarias (IAC), 38200 La Laguna, Tenerife, Spain
[21] Departamento de Astrofísica, Universidad de La Laguna (ULL), La Laguna, Tenerife, Spain
[22] Department of Engineering, University of Cambridge, Cambridge CB3 0FA, UK
[23] Department of Physics & Astronomy, University of British Columbia, 6224 Agricultural Road, Vancouver, BC V6T 1Z1, Canada
[24] European Space Astronomy Centre, PO Box 78, 28691 Villanueva de la Cañada, Madrid, Spain
[25] Institut d'Astrophysique de Paris, 98bis, bd Arago – 75014 Paris, France